

2016

Activation of DNA Pattern Recognition Receptors After Plasmid Electrotransfer in Melanoma Cells and Tumors

Loree Heller
Old Dominion University

Masa Bosnjak

Katarina Znidar

Maja Cemazar

Follow this and additional works at: https://digitalcommons.odu.edu/bioelectrics_pubs

 Part of the [Biomedical Engineering and Bioengineering Commons](#), [Genetic Phenomena Commons](#), and the [Genetic Processes Commons](#)

Repository Citation

Heller, Loree; Bosnjak, Masa; Znidar, Katarina; and Cemazar, Maja, "Activation of DNA Pattern Recognition Receptors After Plasmid Electrotransfer in Melanoma Cells and Tumors" (2016). *Bioelectrics Publications*. 151.
https://digitalcommons.odu.edu/bioelectrics_pubs/151

Original Publication Citation

Heller, L., Bosnjak, M., Znidar, K., & Cemazar, M. (2016). Activation of DNA pattern recognition receptors after plasmid electrotransfer in melanoma cells and tumors. *Molecular Therapy*, 24 Supplement 1, 196-197. doi:10.1016/s1525-0016(16)33304-4

494. Development of a pH Sensor to Probe Endosomal Buffering of Polymeric Nanoparticles Effective for Gene Delivery

David R. Wilson¹, Denis Routkevitch¹, Karl J. Wahlin², Don J. Zack², Alfredo Quinones-Hinojosa³, Jordan J. Green¹

¹Biomedical Engineering, Johns Hopkins University, Baltimore, MD, ²Ophthalmology, Johns Hopkins University, Baltimore, MD, ³Neurosurgery, Johns Hopkins University, Baltimore, MD

Introduction: Polymeric gene delivery suffers from low efficacy compared to viral gene delivery with one of the primary barriers to successful transfection being efficient endosomal escape. Cationic polymers have been hypothesized to facilitate endosomal escape via the proton sponge mechanism by buffering hydrogen ions in the endosomal compartment. Here we have created a nucleic acid based pH sensor and applied it using flow cytometry and confocal microscopy to investigate endosomal buffering of synthetic biodegradable cationic polymers for gene delivery, correlating the pH of delivered DNA with transfection. **Methods:** We created a nucleic acid pH sensor by conjugating pH sensitive (FITC, OG) and insensitive (Cy5) fluorophores to plasmid DNA. The fluorescence ratio of the sensor was calibrated to pH using flow cytometry and confocal microscopy following electroporation into cells. Cells were transfected with the plasmid pH sensor complexed with cationic polymers including poly(beta-amino ester)s (PBAEs) of variable transfection efficacy to investigate endosomal buffering. Additionally, confocal microscopy was used to assess colocalization of the plasmid pH sensor with a lysosomal dye. **Results:** PBAEs were demonstrated to effectively buffer endosomes and avoid lysosomal fate, whereas the negative controls poly-L-lysine (PLL) and polyethylenimine (PEI) were shown to accumulate in lysosomes by 24h post-transfection. The polymer molecular weight and weight-weight ratio to plasmid DNA was shown to have an effect on endosomal buffering as well as transfection efficacy in the case of PBAEs. From confocal microscopy analysis of endosomes, local pH was observed to be higher at the endosomal membrane than in the center, which may be indicative of polymer enrichment along the membrane due to excess soluble polymer. **Conclusions:** The constructed DNA sensor gave a linear relationship with intracellular pH. When investigating PBAE-induced buffering, results were consistent with the hypothesized proton sponge mechanism. These cationic polymers were demonstrated to affect endosomal pH and DNA lysosomal fate and lead to successful transfection.

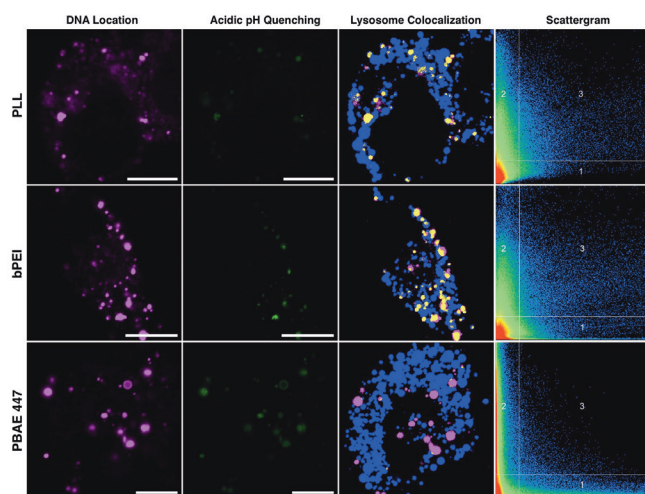


Fig 1: Confocal microscopy was used to assess the compartmental pH of endosomes containing nanoparticles formed with the pH sensor. Lysosome colocalization is shown in merged thresholded images

with lysosomes (blue), DNA non-colocalized with lysosomes (pink) and DNA colocalized with lysosomes (yellow). Scattergrams show DNA fluorescence (horizontal) and lysosome fluorescence (vertical). Scale bar 10 μ m.

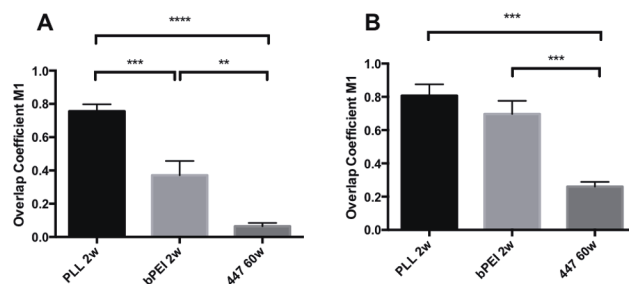


Fig 2. Confocal microscopy images were analyzed at (A) 1 hour and (B) 24 hours post-transfection using Pearson's correlation coefficient M1 to assess the fraction of DNA colocalized with lysosomal stain. When delivered via PBAE 447, the fraction of DNA colocalized with lysosomes was significantly different than both bPEI and PLL at both time points.

495. Activation of DNA Pattern Recognition Receptors After Plasmid Electrotransfer in Melanoma Cells and Tumors

Loree Heller¹, Masa Bosnjak², Katarina Znidar³, Maja Cemazar²

¹Old Dominion University, Norfolk, VA, ²Institute of Oncology Ljubljana, Ljubljana, Slovenia, ³University of Primorska, Izola, Slovenia

In vivo electroporation or electrotransfer, the application of controlled electric pulses, enhances delivery of plasmid DNA to a wide variety of healthy tissues as well as many tumor types. Electrotransfer of pDNA encoding therapeutic genes substantially increases gene expression, enhancing subsequent therapeutic effects. Delivery of therapeutic plasmid DNA has reached clinical trials in the US and in Europe, primarily for cancer therapies and infectious disease vaccines. In several preclinical tumor models, delayed tumor growth, increased survival time, and even complete tumor regression can occur with intratumoral electroporation, also known as electrotransfer, of DNA oligonucleotides or plasmid DNA devoid of a therapeutic gene (empty vector). In B16.F10 mouse melanomas, these effects are preceded by significant elevation of several proinflammatory cytokines and chemokines including IFN β , implicating the binding and activation of intracellular DNA-specific pattern recognition receptors in response to DNA electrotransfer. The purpose of this study was to investigate whether melanoma tumors and cells express cytosolic DNA sensors and whether these sensors respond to pDNA electrotransfer. Histologically, tumor necrosis independent of caspase-3 was observed. Although the mRNAs for several DNA sensors were detected in tumors, none was significantly upregulated. In B16.F10 cells in culture, IFN β mRNA and protein levels were significantly upregulated after pDNA electrotransfer. The mRNAs for several DNA sensors were present in these cells and DAI, DDX60, and p204 mRNAs were significantly upregulated after pDNA electrotransfer. DDX60 protein levels were coordinately upregulated. Mirroring the observation of tumor necrosis, cells underwent a significant pDNA concentration-dependent decrease in proliferation and survival. Taken together, increased IFN β and DNA sensor expression accompanied by cell death and tumor necrosis indicate that pDNA electrotransfer activates intracellular DNA sensors in B16.F10 cells and tumors, producing both *in vitro* and *in vivo* effects. The absence of activation of DNA sensors *in vivo* could be due to the lower transfection efficiency compared to that *in vitro*

or to dilution by other tumor cell types. Electrotransfer is an efficient means of enhancing plasmid DNA introduction into tissues such as skin, muscle, and tumors for therapeutic application. Localized inflammation and induced cell death may contribute to cancer gene therapies but may impede gene therapies for which these effects are not desirable.

496. Elucidating Design Rules Governing Extracellular Vesicle-Mediated Therapeutic Protein Delivery

Michelle E. Hung, Joshua N. Leonard
Chemical and Biological Engineering, Northwestern University, Evanston, IL

Extracellular vesicles (EVs) are secreted biological nanoparticles that have great potential as therapeutic delivery vehicles - they are well-tolerated *in vivo* and naturally capable of transferring RNA and proteins between cells. Our ability to engineer EVs as therapeutic delivery vehicles is limited by an incomplete understanding of how EVs load biomolecular cargo and deliver it to recipient cells. In particular, the biophysical rules governing mRNA and protein delivery by EVs have not been elucidated. Open questions include: Does size limit mRNA loading efficiency into EVs? To what extent is EV mRNA cargo translated in recipient cells? What factors impact the degree to which RNA and protein cargo are delivered to the cytoplasm of recipient cells?

To quantitatively investigate the above questions, we leveraged our Targeted and Modular EV Loading (TAMEL) platform, which enables active loading of specific cargo RNA into EVs. TAMEL can enrich cargo mRNA loading into EVs up to 40-fold relative to passive loading. By directly comparing active loading efficiencies between mRNAs of different lengths, we characterized what type of RNAs can be loaded into EVs. While active loading of mRNA-length (> 1.5 kb) cargo molecules was significant, active loading was much more efficient for smaller (~0.5 kb) RNA molecules, providing the first direct evidence for the impact of cargo RNA size on loading into EVs. We next leveraged the TAMEL platform to elucidate the limiting steps in EV-mediated delivery of mRNA and protein to prostate cancer cells, as a therapeutically relevant model system. In this model system, we did not observe translation of EV-delivered mRNA in recipient cells, indicating this is a limiting step in functional delivery of EV cargo. In contrast, we observed robust EV-mediated delivery of dTomato reporter protein, and thus further explored EVs as therapeutic protein delivery vehicles.

To probe the efficacy of EV-mediated therapeutic protein delivery, we investigated using EVs to deliver the prodrug converting enzyme cytosine deaminase fused to uracil phosphoribosyl transferase (CD-UPRT), which converts the prodrug 5-FC to the toxic 5-FU. Importantly, CD-UPRT can function without requiring endosomal escape because both 5-FC and 5-FU are membrane permeable. We also explored strategies for EV-mediated delivery of Cas9 nuclease, which must overcome the EV loading barrier imposed by its NLS sequence as well as escape the endosome in recipient cells. To address the loading challenge, we investigated a strategy for conditional NLS reconstitution to allow enhanced loading of Cas9 into EVs. We then used Cas9 delivery to assess the degree to which EV-delivered proteins can escape the endosomal/lysosomal pathways and traffic to other subcellular locations. Altogether, our investigations elucidated key design rules and central limiting steps that may guide the further development and utilization of EVs as therapeutic biomolecule delivery vehicles.

Musculo-Skeletal Diseases

497. Follistatin Gene Therapy Improves Six Minute Walk Distance in Sporadic Inclusion Body Myositis (sIBM)

Jerry R. Mendell, Zarife Sahenk, Mark Hogan, Samiah Al-Zaidy, Kevin Flanigan, Louise R. Rodino-Klapac, Markus McColly, Kathleen Church, Sarah Lewis, Linda Lowes, Lindsay Alfano, Katherine Berry, Natalie Miller, Igor Dvorchik, Melissa Moore-Clingenpeel, Brian K. Kaspar
Gene Therapy, The Research Institute at Nationwide Children's Hospital, Columbus, OH

Treatment of sIBM poses many challenges. The cause of this disease is enigmatic, and although considered to be an inflammatory myopathy, there is resistance to anti-inflammatory and immunosuppressive agents. sIBM muscle biopsies show vacuolated muscle fibers, widespread inflammation, and intracellular amyloid deposits. Follistatin is a potent inhibitor of the myostatin pathway and its potential as a therapeutic vehicle is enhanced by a pathway independent of the activin IIB receptor. We have demonstrated both safety and efficacy following direct intramuscular injection of follistatin in the quadriceps muscle in a previously reported gene therapy trial in Becker muscular dystrophy (Mendell JR, et al Mol Ther 2015). No off target effects were encountered attributed to the use of an alternatively spliced follistatin isoform, FS344, also used in the current sIBM gene therapy trial. Enrollment in the current gene therapy trial included 6 subjects with either definite or possible sIBM (Griggs RC, et al. Ann Neurol 1995). Pretreatment MRI's were obtained to determine areas of relative muscle sparing/lack of fibrosis. The intramuscular injections of AAV1.CMV.FS344 to 12 to 14 sites in the quadriceps muscle delivered 1.2×10^{12} vg/kg. Injections were performed with direct ultrasound guidance to target the most normal appearing muscle bundles, and intramuscular position was confirmed with simultaneous EMG. A three-patient, single limb, safety trial preceded the Phase I/IIA trial reported here. During the ongoing gene therapy trial, a control sIBM group (n=20) was prospectively studied by performance of the 6MWT with follow up from 9-28 months.

The 6MWT was the primary functional outcome (See table below). sIBM patients treated with AAV1.CMV.FS344 increased the 6MWT distance by 46.5m (457 to 503.5, p=0.001). Untreated sIBM controls lost 38.5m over a similar time period resulting in net difference of 85.0m between groups (p=0.0007). To validate findings and confirm the lack of selection bias we compared a subgroup of untreated sIBM controls (n=8), matched for age, gender, and 6MWD at baseline. Matched controls lost 39m (p=0.0036) in the 6MWT, a virtually identical loss to the larger control group.

The results of this study demonstrate that sIBM can benefit from follistatin gene therapy based on improvement in distance walked in the 6MWT. We did find a hierarchy of response based on muscle preservation and avoiding gene delivery to areas of fibrosis. In this study, gene delivery was limited to the quadriceps muscle, but in future trials more widespread delivery could potentially be more effective.

Six Minute Walk Distance Pre- and Post-Treatment* [median values (interquartile ranges provided)]				
Group	Baseline (m)	Final Compared to Baseline (m)	Change from Baseline (m)	Change per Month (m)
sIBM Gene Therapy Pts (n=6)	457 (431,475)	Improved to 503.5 (443,573)	+46.5 (2,117)	+3.09 (0.39,8.9)
Untreated sIBM Controls (n=20)	393 (356.5,451.5)	Declined to 354.5 (303.5,410.5)	-38.5 (-73,-22) p=0.0007	-2.3 (-4,-1.1) P=0.0032
Matched sIBM Controls for age, gender, and 6MWD (n=8)	459 (439.5,469)	Declined to 420 (388.5,447.5)	-39.0 (-77,-8) p=0.0036	-2.2 (-4.8,-0.7) P=0.0118